Temporal and spatial variability of the oceanic front between the Atlantic Water and adjacent water masses north of Svalbard

Stian Vikanes [1 2] Frank Nilsen [1 2] Ragnheid Skogseth [1]

[1]The University Centre in Svalbard [2]University of Bergen

Introduction

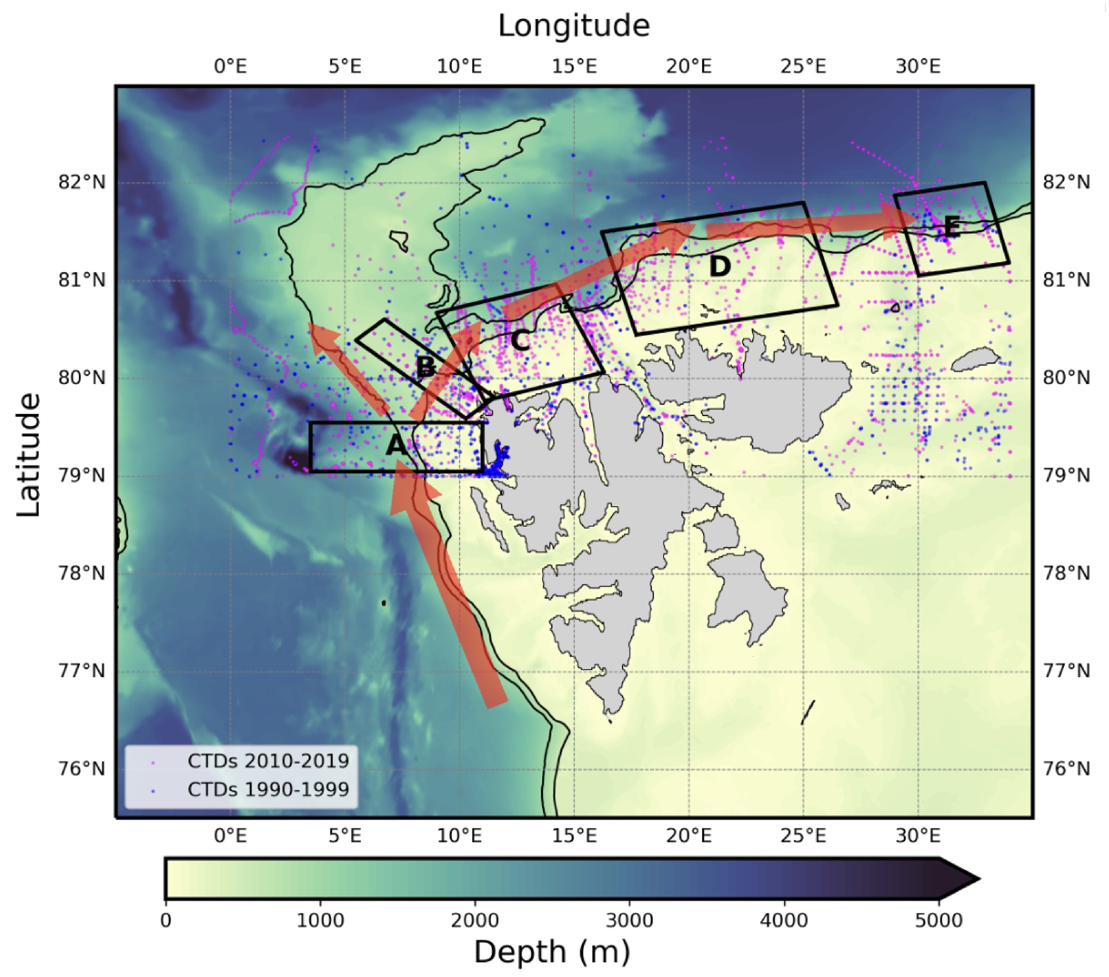

Figure 1. An overview of the study area. Rectangles labeled A through E represent the regions where climatological sections are constructed. Red arrows depict the pathway of the West Spitsbergen Current (WSC) along the shelf slope west and north of Svalbard. The ocean bathymetry is from the International Bathymetric Chart of the Arctic Ocean [Jakobsson et al., 2012]. The 500 and 1000 m contours are plotted, but not labeled. Magenta and blue dots represent locations of CTD profiles and show the data coverage for the decades 2010-2019 and 1990-1999, respectively.

The inflow of warm and saline Atlantic Water (AW) into the Arctic Ocean is influenced by oceanic fronts and air-ice-sea interactions west and north of Svalbard. The AW is shown to have a significant impact on the sea ice extent and marine ecosystems in the region. Understanding the variability of oceanic fronts related to AW inflow into the Arctic and how it is related to the atmosphere and sea ice is therefore of public significance.

In this study, we use historical and more recent hydrographic data to analyze and describe the variability of surface and subsurface fronts in terms of dominant water masses and their location along the continental slope north of Svalbard.

Data & Methods

Data: Hydrographic data from the UNIS Hydrographic Database [Skogseth et al., 2019] are accompanied with additional data from the Norwegian Marine Data Centre. The data used in this work are from the areas depicted in Figure 1 for the period 1980 to 2022.

Methods:

- Define suitable locations for Sections A-E based on data availability and previous studies [E.g. Saloranta and Haugan, 2001, Cokelet et al., 2008, Koläs and Fer, 2018].
- Weighted bin averaging and interpolation of data points along Sections A-E to gain fine grids of potential temperature (Θ) and absolute salinity (S_A).
- Sort the densities and run the grids through a uniform filter to reduce high frequency noise.
- Averaged values of potential temperature and absolute salinity are restricted to the layers 0-100m, 100-500m and 0-500m with a horizontal extent from 35 km on-shelf to 50 km off-shelf relative to the shelf break.

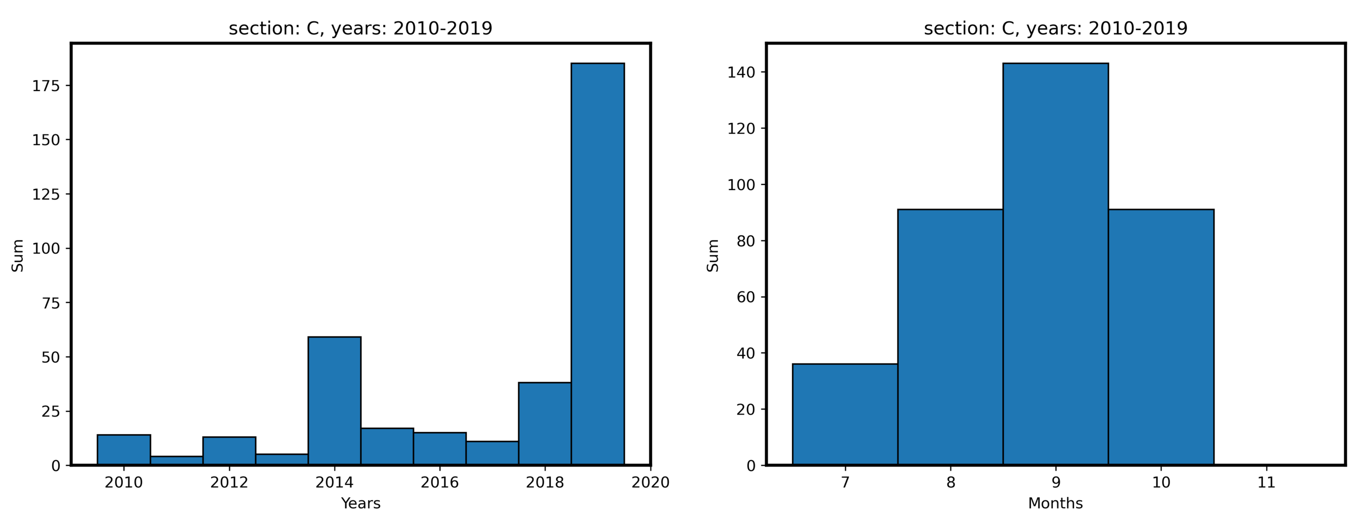

Sharing is encouraged

(a) Histogram showing the distribution of profiles over years and months obtained in Section C for the decade 2010-2019.

Results

- Hydrographic decadal climatologies from Sections A-E along the WSC (Figure 3)
- Water mass transformations along the WSC (Figure 3)
- Calculated heat fluxes along the pathway of the WSC (Table 1), based on Eq. 1.
- The evolution of both mean and maximum potential temperature and absolute salinity over time and space, including their respective pressure levels (Figure 4) based on bin averaged sections before smoothing.
- $\Theta - S_A$ diagrams based on bin averaged sections before smoothing (Figure 5) better visualize the water masses and their transformations. Red stippled mixing lines based on different ratios between heat flux to the atmosphere and sea ice melt are included.

Table 1. Calculated heat fluxes, W m^{-2}, from different depth layers of the WSC.

	Layer	1980-1989	1990-1999	2000-2009	2010-2019	2020-2022	Average
	0-100	-430	-80	-120	-240	NaN	-220
A-C	100-500	-430	-290	-245	-335	NaN	-325
	0-500	-925	-405	-390	-600	NaN	-585
	0-100	-225	-330	-190	-220	-120	-215
C-E	100-500	-95	-140	-30	-110	-45	-85
	0-500	-275	-495	-210	-310	-155	-285
	0-100	-455	-365	-180	-385	-635	-400
D-E	100-500	-335	-270	-120	-205	-495	-290
	0-500	-650	-575	-275	-560	-1135	-640
	0-100	-280	-275	-195	-240	NaN	-250
A-E	100-500	-170	-170	-85	-175	NaN	-150
	0-500	-420	-470	-270	-405	NaN	-390

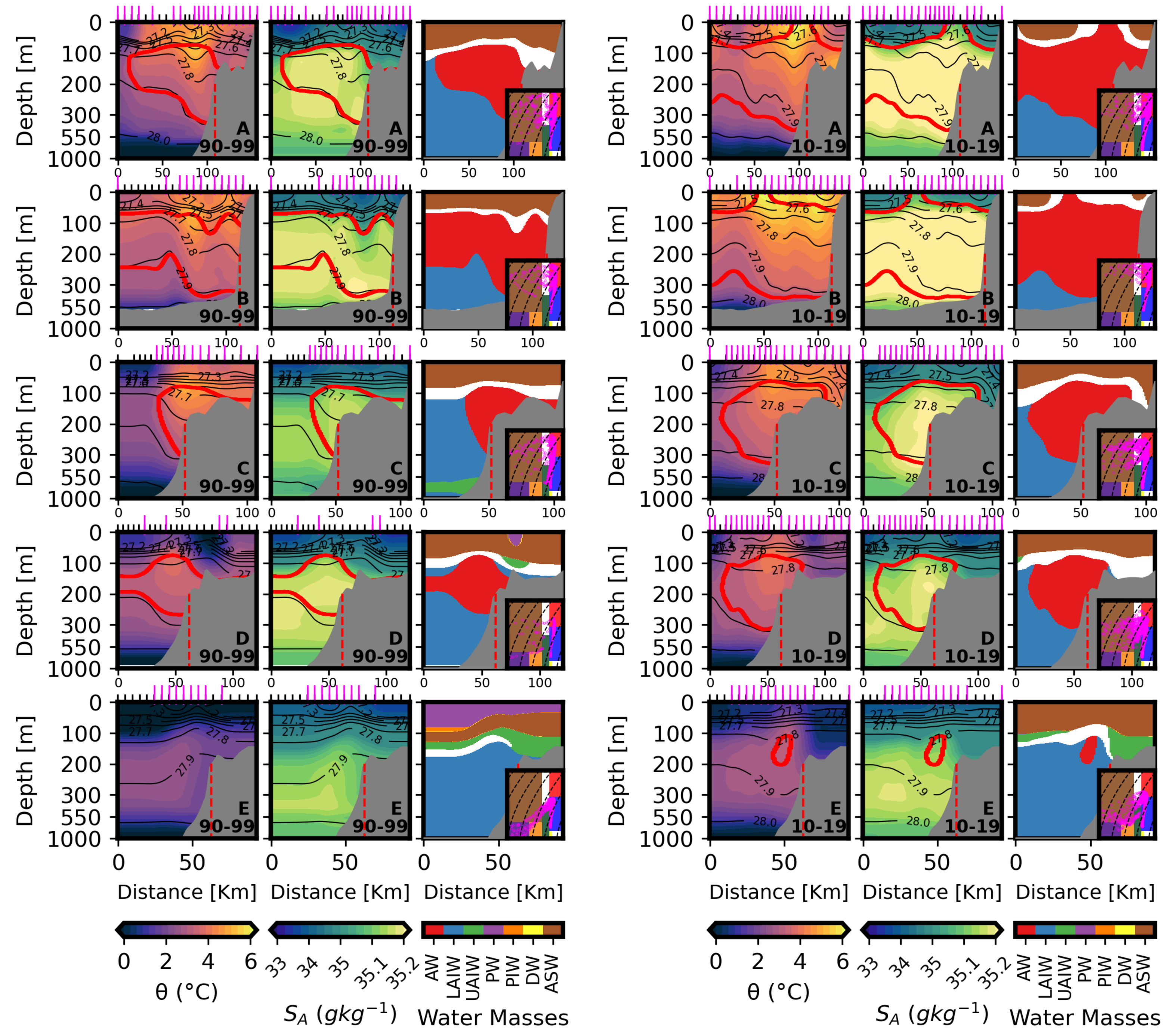

Figure 3. Hydrographic (Θ and S_A) decadal climatologies from Sections A through E are presented from decades 1990-1999 (left) and 2010-2019 (right). The magenta lines on top of the panels show where we have enough observations for the bin average. The red contours indicate the AW. The last column shows the dominant water masses with a corresponding $\Theta - S_A$ diagram for reference in the lower right corner. The vertical resolution is linear until 300 m and logarithmic below. The absolute salinity scale changes resolution after 35 g kg^{-1}. The shaded grey areas illustrate the bottom topography.

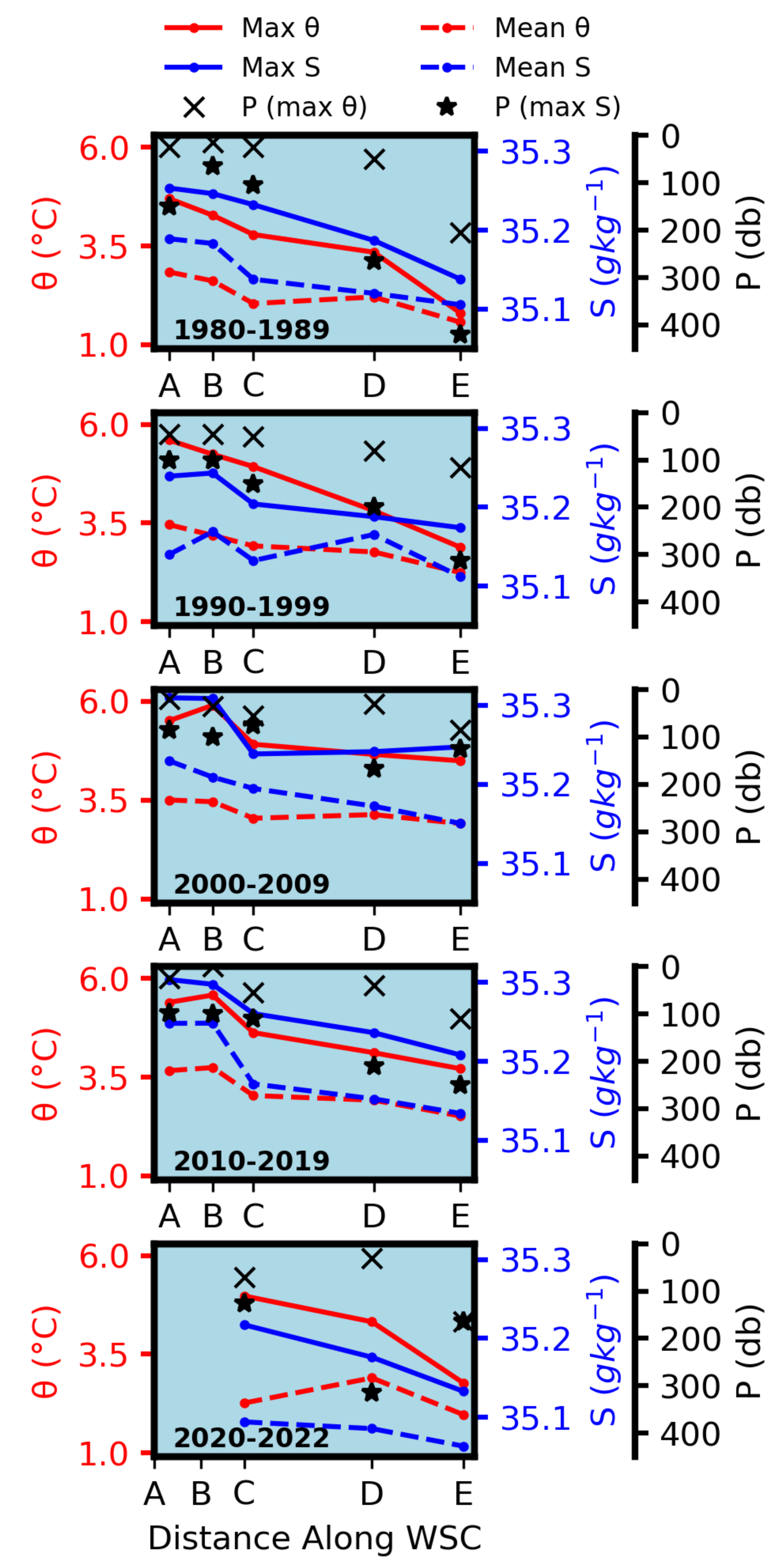

Figure 4. Evolution of potential temperature and absolute salinity.

$$\int_{Surface} (Q+H)dxdy = \rho_0 C_p \bar{v} \int_A \frac{\partial \overline{T}}{\partial y} dxdz, \qquad (1)$$

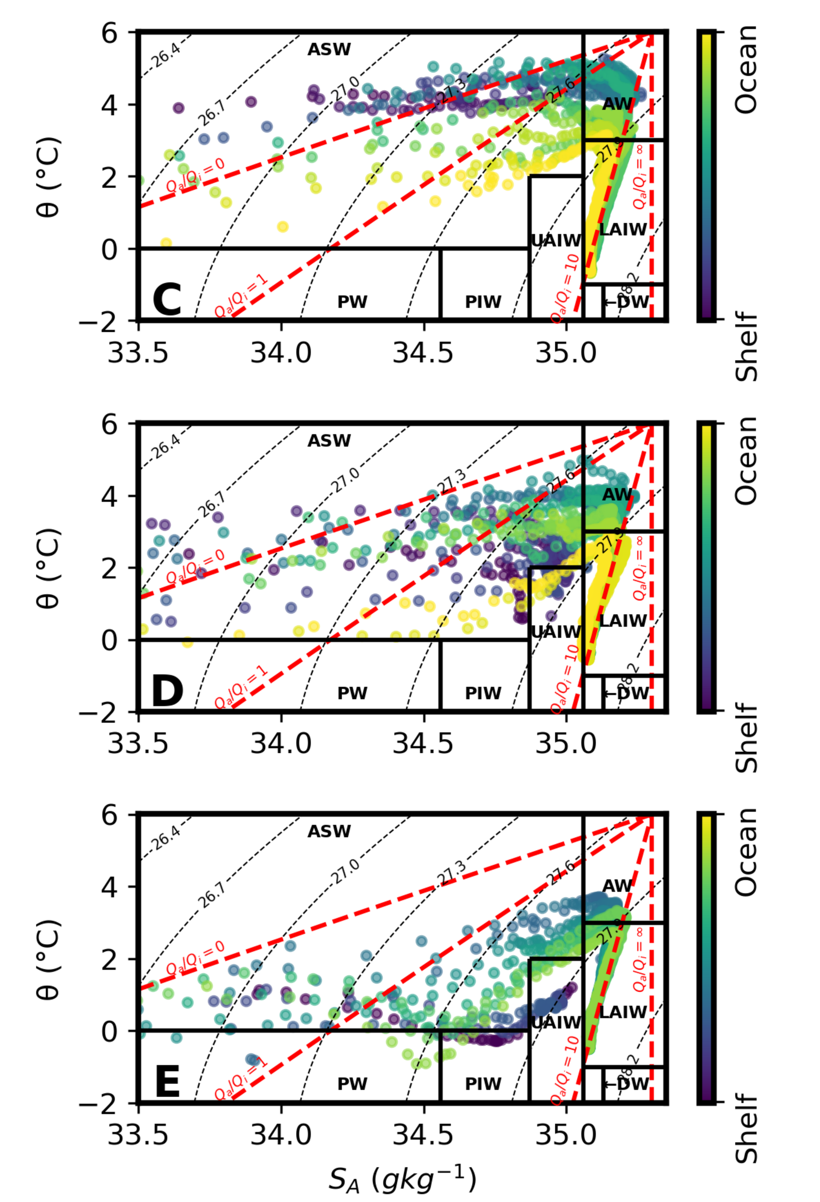

Figure 5. $\Theta - S_A$ diagrams from 2010-2019 for Sections C, D and E. Stripled lines based on ratios between heat flux to atmosphere or sea ice.

Discussion

- 2000-2009 seems to be an anomalously warm and saline decade. Mean Θ and S_A at Section E is found to be 2.91°C and 35.15 gkg^{-1}. Table 1 suggests that this decade had relatively low heat fluxes, potentially because of higher air temperatures?
- 2020-2022 seems to be a cold anomaly. Mean Θ and S_A at Section E is found to be 1.97°C and 35.06 gkg^{-1}. Similar results by Kolås et al. [2023] in the Barents Sea.
- The $\Theta - S_A$ diagram from Section E suggests equal heat flux to atmosphere and sea ice melt, while in Sections C and D sea ice melt (and potentially other freshwater sources) dominates, contradictory to Cokelet et al. [2008].
- $\Theta - S_A$ diagrams suggest that sea ice melt dominates above the AW, while offshore and onshore of the AW atmospheric cooling gets more significant.

References

E. D. Cokelet, N. Tervalon, and J. G. Bellingham. Hydrography of the West Spitsbergen Current, Svalbard Branch: Autumn 2001. *Journal of Geophysical Research: Oceans*, 113(1), 1 2008. ISSN 21699291. doi: 10.1029/2007JC004150.

M. Jakobsson, L. Mayer, B. Coakley, J. A. Dowdeswell, S. Forbes, B. Fridman, H. Hodnesdal, R. Noormets, R. Pedersen, M. Rebesco, H. W. Schenke, Y. Zarayskaya, D. Accettella, A. Armstrong, R. M. Anderson, P. Bienhoff, A. Camerlenghi, I. Church, M. Edwards, J. V. Gardner, J. K. Hall, B. Hell, O. Hestvik, Y. Kristoffersen, C. Marcussen, R. Mohammad, D. Mosher, S. V. Nghiem, M. T. Pedrosa, P. G. Travaglini, and P. Weatherall. The International Bathymetric Chart of the Arctic Ocean (IBCAO) Version 3.0. *Geophysical Research Letters*, 39(12), 6 2012. ISSN 00948276. doi: 10.1029/2012GL052219.

E. Koläs and I. Fer. Hydrography, transport and mixing of the West Spitsbergen Current: The Svalbard Branch in summer 2015. *Ocean Science*, 14(6):1603–1618, 12 2018. ISSN 18120792. doi: 10.5194/OS-14-1603-2018.

E. H. Kolås, T. M. Baumann, R. Skogseth, Z. Koenig, and I. Fer. Western Barents Sea Circulation and Hydrography, past and present. Technical report, 2023.

T. M. Saloranta and P. M. Haugan. Interannual variability in the hydrography of Atlantic water northwest of Svalbard. *Journal of Geophysical Research: Oceans*, 106(C7):13931–13943, 7 2001. ISSN 21699291. doi: 10.1029/2000JC000478.

R. Skogseth, P. Ellingsen, J. Berge, F. Cottier, S. Falk-Petersen, B. Ivanov, F. Nilsen, J. Søreide, and A. Vader. UNIS hydrographic database [Data set]. *Norwegian Polar Institutes*, 2019. doi: https://doi.org/10.21334/unis-hydrography.

https://doi.org/10.5194/egusphere-egu24-10445 EGU General Assembly 2024 107257@student.unis.no